Perturbations of Heart Development and Function in Cardiomyocytes from Human Embryonic Stem Cells with Trisomy 21

Alexis Bosman, Audrey Letourneau, Laura Sartiani, Martina Del Lungo, Flavio Ronzoni, Rostyslav Kuziakiv, Virpi Tohonen, Marco Zucchelli, Federico Santoni, Michel Guipponi, Biljana Dumevska, Outi Hovatta, Stylianos E. Antonarakis, Marisa E. Jaconi

Perturbations of Heart Development and Function in Cardiomyocytes from Human Embryonic Stem Cells with Trisomy 21

ALEXIS BOSMAN,[a,b] AUDREY LETOURNEAU,[c] LAURA SARTIANI,[d] MARTINA DEL LUNGO,[d]
FLAVIO RONZONI,[a] ROSTYSLAV KUZIAKIV,[a] VIRPI TOHONEN,[e] MARCO ZUCCHELLI,[e]
FEDERICO SANTONI,[c] MICHEL GUIPPONI,[c] BILJANA DUMEVSKA,[f] OUTI HOVATTA,[g]
STYLIANOS E. ANTONARAKIS,[c,h] MARISA E. JACONI[a]

[a]Department of Pathology and Immunology, Faculty of Medicine and [c]Department of Genetic Medicine and Development, Faculty of Medicine, University of Geneva, Geneva, Switzerland; [b]Victor Chang Cardiac Research Institute, Darlinghurst, New South Wales, Australia; [d]Department of Neuroscience, Psychology, Drug Research and Child Health, Center of Molecular Medicine, University of Florence, Florence, Italy; [e]Department of Biosciences and Nutrition, Karolinska Institute, Huddinge, Sweden; [f]Genea Biocells, Sydney, New South Wales, Australia; [g]Division of Obstetrics and Gynecology, Department of Clinical Science, Karolinska Institute, Huddinge, Stockholm, Sweden; [h]iGE3 Institute of Genetics and Genomics of Geneva, Geneva, Switzerland

Correspondence: Marisa Jaconi, Ph.D., Department of Pathology and Immunology, Faculty of Medicine, Geneva University, 1 rue Michel-Servet, 1211 Geneva 4, Switzerland. Telephone: +41-22-379-5257; e-mail: marisa.jaconi@unige.ch or Alexis Bosman, Ph.D., Victor Chang Cardiac Research Institute, 405 Liverpool St, Darlinghurst, 2010 NSW, Australia. Telephone: +61-432494777; e-mail: a.bosman@victorchang.edu.au

ABSTRACT

Congenital heart defects (CHD) occur in approximately 50% of patients with Down syndrome (DS); the mechanisms for this occurrence however remain unknown. In order to understand how these defects evolve in early development in DS, we focused on the earliest stages of cardiogenesis to ascertain perturbations in development leading to CHD. Using a trisomy 21 (T21) sibling human embryonic stem cell (hESC) model of DS, we show that T21-hESC display many significant differences in expression of genes and cell populations associated with mesodermal, and more notably, secondary heart field (SHF) development, in particular a reduced number of $ISL1^+$ progenitor cells. Furthermore, we provide evidence for two candidate genes located on chromosome 21, ETS2 and ERG, whose overexpression during cardiac commitment likely account for the disruption of SHF development, as revealed by downregulation or overexpression experiments. Additionally, we uncover an abnormal electrophysiological phenotype in functional T21 cardiomyocytes, a result further supported by mRNA expression data acquired using RNA-Seq. These data, in combination, revealed a cardiomyocyte-specific phenotype in T21 cardiomyocytes, likely due to the overexpression of genes such as RYR2, NCX, and L-type Ca^{2+} channel. These results contribute to the understanding of the mechanisms involved in the development of CHD. STEM CELLS 2015;33:1434–1446

INTRODUCTION

Down syndrome (DS) is the most common human chromosomal disorder which occurs in approximately 1 in 750 of live births [1, 2]. It is caused by the presence of all or part of an extra human chromosome 21 (HSA21) [3]. Common traits present in all individuals include mental retardation, reduced brain size, impaired long-term memory, and cranio-facial alterations [4]. While abnormalities such as congenital heart defects (CHD) only occur in approximately 40%–50% of DS individuals [5, 6], they represent the leading cause of morbidity.

Despite the cause of DS being known for decades, the underlying mechanisms for the aforementioned pathologies associated with DS are not yet well-understood. While it is known that gene-dosage imbalances disrupt development, the exact mode of action of these imbalances and the cellular pathways involved remain to be clearly ascertained [7]. To date, there have been a small number of studies into the transcript and protein expression of cells from trisomic tissues, giving only an indication of the molecular pathways involved in the pathologies of the disease [8–11]. Current methods using human trisomic tissues are restricted because of practical and ethical reasons, and the limited proliferation capabilities of cardiac tissue samples preclude in-depth developmental studies. To date, a number of human stem cell models have been established examining the development of the particular cellular pathways involved in the neural and hematopoietic pathologies associated with trisomy 21 [12–16]. While none have yet definitively identified the underlying cause of the cardiac defects observed in DS, recent studies underline the potential copy number variation (CNV) association with the risk of heart defects [5, 17].

In this study, we report the derivation of one human embryonic stem cell (hESC) line exhibiting complete trisomy 21, and in addition, two euploid lines from the same donor couple, making the three hESC lines "fraternal

siblings." Additionally, we report on a second genetically unrelated hESC line, also exhibiting complete trisomy 21. As it is known that different hESC lines have different differentiation capacities due to differences in genetic background [18], the use of this unique trio of sibling hESC lines significantly reduces the interline variability seen between lines derived from unrelated embryos. This is important in an in vitro modeling setting for complex diseases such as DS, as it allows the differences in differentiation capacities/phenotypes to be directly attributed to the extra copy of HSA21, as opposed to their different genetic backgrounds.

Using our hESC-based model of DS, we investigated gene and protein expression, both over a time course of early development and specifically in cardiomyocytes. Investigations also included functional studies and deep sequencing in isolated beating cardiomyocytes. Using these methods, we show a clear perturbation in the expression of numerous cardiac-associated genes involved in early cardiac differentiation, secondary heart field (SHF) development, and in CHD-associated genes. Furthermore, we identified two genes located on HSA21, ETS2, and ERG, which may be responsible for these observed CHD. Finally, we report an abnormal electrophysiological phenotype of differentiated cardiomyocytes from T21-hESC, similar to that seen in early fetal echocardiograms [19]. This finding was further supported by the mRNA expression data acquired using RNA-Seq. Together, our analyses provide insight into the complex developmental patterns at the basis of CHD in DS.

MATERIALS AND METHODS

Embryo Donation and ESC Derivation and Culture

Donated embryos were originally created by assisted reproduction technologies for the purpose of procreation and cultured to the blastocyst stage as described elsewhere [20]. Embryos described in this study were of poor quality, therefore unsuitable for clinical use and declared as excess to reproductive needs and donated for investigation. All relevant clinical procedures and research protocols were in compliance with the U.S. National Academies' 2008 Guidelines for Human Embryonic Stem Cell Research and were approved by the Genea Ethics Committee, an independent committee constituted according to the requirements of Australia's National Health and Medical Research Council (NHMRC). Derivation and culture of hESC lines was performed as previously described [21], and the lines obtained were designated as GENEA021, GENEA022, GENEA023, and GENEA053, further abbreviated to GEN021, GEN022, GEN023, and GEN053, respectively. Cell lines were imported to Switzerland after approval and authorization from the Swiss Federal Office of Health (OFSP # 2-0001, www.bag.admin.ch). Methods for cell culture were adapted from [22, 23].

Single Nucleotide Polymorphism Array

Genotyping was performed using the Affymetrix Genome-Wide Human SNP Array 6.0 (San Diego, CA, http://www.affymetrix.com/). Labeling and hybridization followed the protocols and kits provided by the manufacturer (Affymetrix Genome-Wide Human SNP Nsp/Sty Assay Kit 5.0/6.0). A set of 50 arrays previously hybridized and genotyped in the same laboratory was used as the copy number neutral reference sample. CNVs and loss of heterozygosity (LOH) were extracted with the Affymetrix proprietary Genotyping Console Software, using the standard setup recommended by the producer. Variations were annotated using the libraries supplied by Affymetrix (version 29). Genes were annotated to the CNVs using the biomart database (www.biomart.org).

Methylation Analysis

Genome-wide methylation array was performed using Infinium HumanMethylation450 Beadchip kit, as per manufacturer's instructions http://www.illumina.com/. Further information about the validation of this product can be seen in [24]. SD and CpG (CG) island filters were applied upon data analysis. Genomic DNA was extracted using GenElute Mammalian Genomic DNA Miniprep Kit (Sigma, https://www.sigmaaldrich.com/).

High Throughput mRNA Sequencing

At day 60 of differentiation, beating cardiomyocyte clusters from each cell line (GEN021, GEN022, GEN023, and GEN053) were manually excised by microdissection using a pulled glass pipette under a stereomicroscope. Clusters were taken from repeated experiments (at least five) with an average of five beating clusters per experiment per cell line. RNA was extracted from pooled clusters using the miRNeasy kit (Qiagen, Hilden, Germany, http://www1.qiagen.com), as per the manufacturer's instructions. mRNA-Seq libraries were prepared from 500 ng of total RNA after size selection using the IlluminaTruSeq RNA Sample Preparation kit (Illumina RS-930–2001), as per the manufacturer's instructions. Libraries were sequenced in two lanes of the Illumina HiSeq 2000 instrument. The 100 bp paired-end reads generated by the machine were mapped against the human genome (hg19) using the default parameters of the Burrows-Wheeler Aligner [25]. For each gene, exon coverage was calculated using a custom pipeline and then normalized in reads per kilobase per million (RPKM). The clustering and principal component analyses (PCA) based on the RPKM values were performed using R (version 2.14.0). EdgeR [26] (version 3.0.7, common dispersion estimate) and DESeq [27] (version 1.10.1, dispersion estimate based on the "fit-only" model) packages were used to assess the differential expression between the trisomic and the euploid samples. Only the genes with more than one read per million in at least three samples were conserved for the analysis. A gene was considered differentially expressed if the FDR (false discovery rate) corrected p value given by both EdgeR and DESeq was lower than .01. The functional annotation analysis of the differentially expressed genes was performed using DAVID (Database for Annotation, Visualization and Integrated Discovery) [28].

Electrophysiological Recordings

Spontaneously beating clusters were dissected using a microscalpel and placed on the gelatin-coated bottom of a perfusion chamber. Intracellular recordings were performed using a standard electrophysiological technique as described previously [29].

Knockdown and Overexpression Studies

Undifferentiated hESC line GEN021 was used for the siRNA knockdown study and GEN023 for the overexpression study.

Cells were passaged to feeder-free conditions, as described previously and transfected with Lipofectamine 2000 as per the manufacturer's instructions. siRNA knockdown was performed with reagents obtained from Santa Cruz (Santa Cruz, CA, http://www.scbt.com; siERG: sc-35333; siETS2: sc-37855 or Life Technologies (Rockville, MD, http://www.lifetech.com; Stealth RNAi siRNA Negative Control Med GC Duplex #3: 12935-113). Plasmids used for overexpression (pERG: pCEFL-HA-ERG3, pETS2: pSGK-ETS2) were a kind gift from Dr. Carlo Catapano (IOR Institute of Oncology Research, Switzerland).

RESULTS

Characterization of hESC Lines

We first confirmed the pluripotent characteristics of the two trisomy 21 hESC lines (GEN021 and GEN053), which displayed similar pluripotent characteristics both in vitro and in vivo when compared to euploid lines (GEN022 and GEN023—siblings of GEN021) (Fig. 1; Supporting Information Fig. S1). Furthermore, each line produced beating cardiomyocyte clusters (Supporting Information Movies S1–S4), with comparable expression of myosin light chain-2a (Mlc2a/MYL7) and of the transcription factor myocyte enhancer factor 2 (MEF2) (Supporting Information Fig. S1), indicating cardiogenic recapitulation in vitro. It was observed that one T21-hESC line (GEN021) produced significantly more observable beating clusters (61.1 ± 7.9) than its siblings GEN022 and GEN023 $(36.1 \pm 6.8\%$ and $35.4 \pm 7.8\%)$, or the other unrelated hESC-T21 line, GEN053 $(21.9 \pm 4.7; p < .05, n = 6$ independent experiments).

Due to the observed variations in differentiation efficiencies between hESC lines reported in the literature [18], we hypothesized that using cell lines from genetically similar backgrounds would reduce this variability. Using SNP genotyping, we thus ascertained genomic similarities between the hESC lines. As expected, our three sibling lines (GEN021, GEN022, GEN023) were highly genetically similar in relation to their SNPs (∼77% concordance) in contrast to the genetically unrelated trisomic line GEN053, observed to be appreciably different (∼62% concordance). CNVs were additionally examined in each cell line (Supporting Information Fig. S2), identifying a very small number of differences between lines. The structural variations (deletions or insertions) uncovered by this analysis were not reported to be involved in early cardiogenesis.

As epigenetic properties, such as DNA methylation, are also known to influence the differentiation capacities of pluripotent stem cells further contributing to the interline variation observed in differentiation studies [30], we next examined whole genome DNA methylation patterns of each hESC line. Global epigenomic similarities between the cell lines can easily be observed from the methylation heat map in relation to the pluripotency- and early development-associated genes (Fig. 1C). Upon calculation of the Pearson's correlation, we detected a highly similar methylation pattern between the lines (∼94% similarity for all lines; Supporting Information Table S1). However, the methylation pattern of five well-known pluripotency genes (NANOG, OCT4, SOX2, REX1, LIN28) was less uniform (Fig. 1E), despite the highly similar mRNA expression levels for those pluripotency genes (Fig. 1D). Interestingly, although REX1 appeared to be more

methylated in GEN021 (Fig. 1E), its mRNA expression level was not significantly reduced.

Examination of Cardiac Development and Differentiation

To uncover possible perturbations in the expression patterns of key genes involved in both early cardiogenesis and in CHD (Supporting Information Table S1), we differentiated all hESC lines to embryoid bodies (EBs). We examined by quantitative polymerase chain reaction (qPCR) the expression of cardiac-associated genes characteristic of the (a) mesoderm/pre-cardiac, (b) first heart field (FHF), (c) FHF/SHF, and (d) SHF, in whole EBs collected at specific time points of development. Firstly, both T21 lines (GEN021 and GEN053) showed a significantly reduced level of the early mesodermal marker BRACHYURY $(p < .05)$ compared to euploid lines (GEN022 and GEN023) (Fig. 2A). The early pre-cardiac marker MESP1 was also downregulated, however only in GEN021. In regards to β-catenin (CTNNB1), known to be necessary for the proliferation and development of pre-cardiac mesoderm and cardiac mesoderm, we detected a significantly lower expression in GEN021 at d4, which continued as a trend up until d21 in both T21-hESC lines (GEN021 and GEN053) (Fig. 2B). Moreover, WNT3A, which plays an important role in early cardiogenesis, was also reduced in GEN053 (Fig. 2B). These results indicate that at the earliest stages of mesodermal development and cardiogenesis, a perturbation is already observed in T21-hESC in comparison to euploid hESC.

We then examined possible differences at later points in cardiac differentiation, specifically cardiac specification during the development of the two heart fields. First, HAND1 and MEF2C, key genes involved in the FHF were not differentially expressed (Fig. 2C). However, when examining genes associated with both the FHF/SHF, specifically GATA4, NOTCH1, NKX2–5, and TBX20, we observed many significant differences in expression levels between the T21-hESC and the euploid hESC (Fig. 2D). Of particular interest, GATA4 was significantly overexpressed at d8 in both the T21-hESC, while GEN021 exhibited a significantly reduced level of expression of NKX2–5 at d4. Additionally, NOTCH1 was also significantly less expressed at all three time points (d4, 8, 21) in GEN021, with TBX20 also significantly less expressed at d4 in both T21-hESC. Key genes associated with SHF development, specifically ISL1, WNT11, FGF10, HAND2, and TBX1, showed several important differences between the T21-hESC and the euploid hESC. Of most significant relevance is the differential expression of both ISL1 and WNT11. ISL1, a master regulator in the development of the SHF, was greatly reduced both d4 and d8 in both T21 lines, while WNT11 was increased at d21 in both T21 lines with TBX1 reduced only in GEN021 at d4 (Fig. 2E). We next confirmed by fluorescence-activated cell sorting (FACS) that the number of $ISL1^+$ and $GATA4^+$ cells was indeed reduced and increased, respectively, in both the T21-hESC lines $(n = 3, p < .05;$ Fig. 2F), correlating well with the mRNA expression data (Fig. 2D, 2E). These combined results, along with further examinations of other genes involved in cardiovascular development (Supporting Information Fig. S7), show complex yet clear and significant perturbations in expression of genes and proteins associated with early heart development in the T21-hESC.
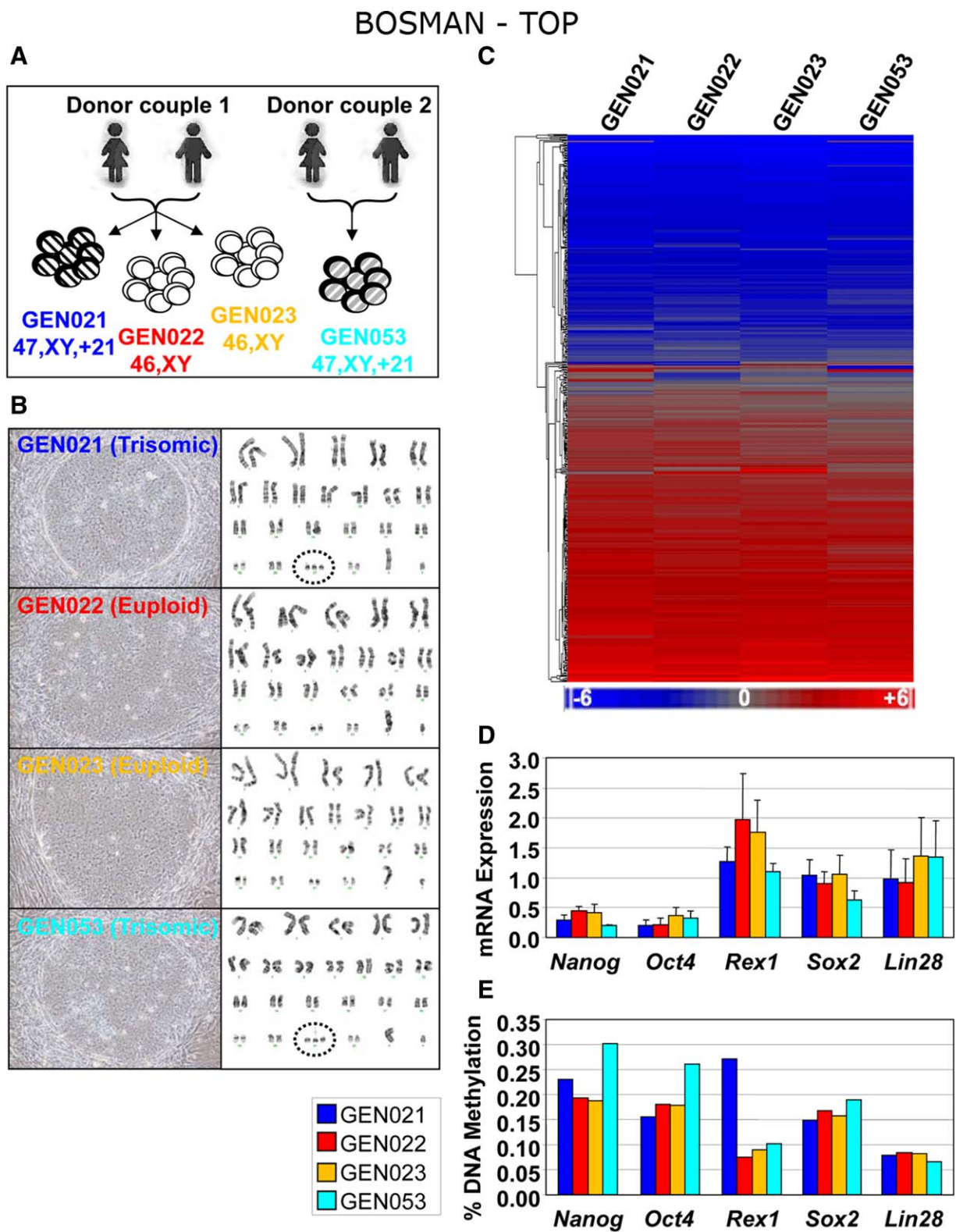
BOSMAN - TOP

Figure 1. Pluripotent stem cell based model of Down syndrome (DS) using human embryonic stem cell (hESC) exhibiting T21 and sibling controls. **(A):** Graphic representing the hESC DA model. **(B):** Phase contrast images (×100) of undifferentiated colonies from all hESC lines and their representative karyotypes. **(C):** Heat map exhibiting DNA methylation patterns of genes associated with pluripotency and early development. **(D):** mRNA expression of pluripotent genes. **(E):** DNA methylation percentages at pluripotent genes. See also Supporting Information Figures S1, S2.
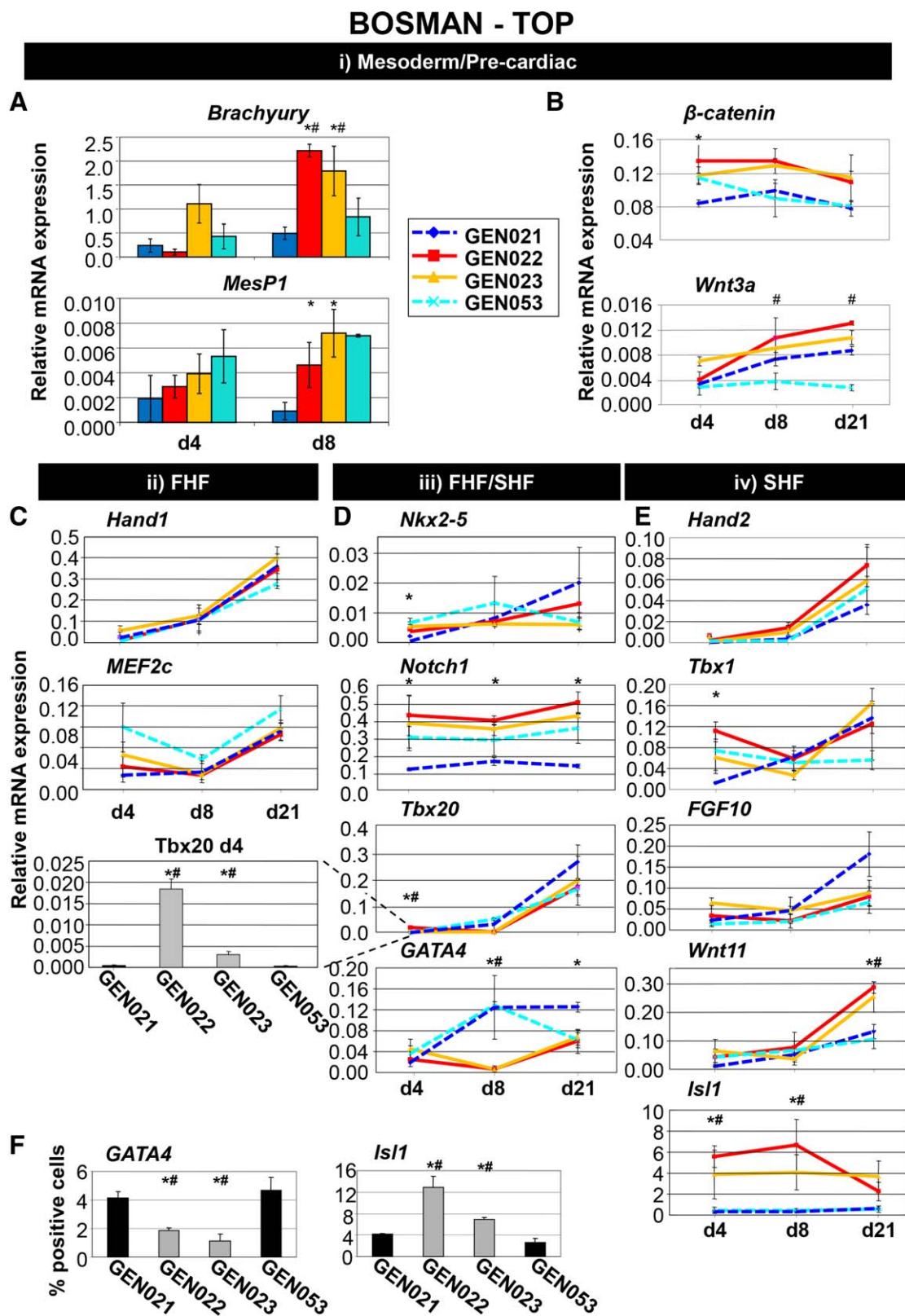
Figure 2. Time course of mRNA expression of genes associated with cardiac development. **(A):** Expression of mRNA in genes associated with mesodermal development. ($n = 3–4$). **(B):** Expression of mRNA in genes associated with pre-cardiac development ($n = 3–4$). **(C):** mRNA expression of genes associated with FHF ($n = 3–4$). **(D):** mRNA expression of genes associated with FHF/SHF ($n = 3–4$). **(E):** mRNA expression of genes associated with SHF ($n = 3–4$). **(F):** Comparison of cell populations by fluorescence-activated cell sorting at d8 of differentiation expressing either ISL1 or GATA4 ($n = 3$). Scheme: * $p < .05$ (comparison to GEN021); #, $p < .05$ (comparison to GEN053). Abbreviations: FHF, first heart field; SHF, secondary heart field.
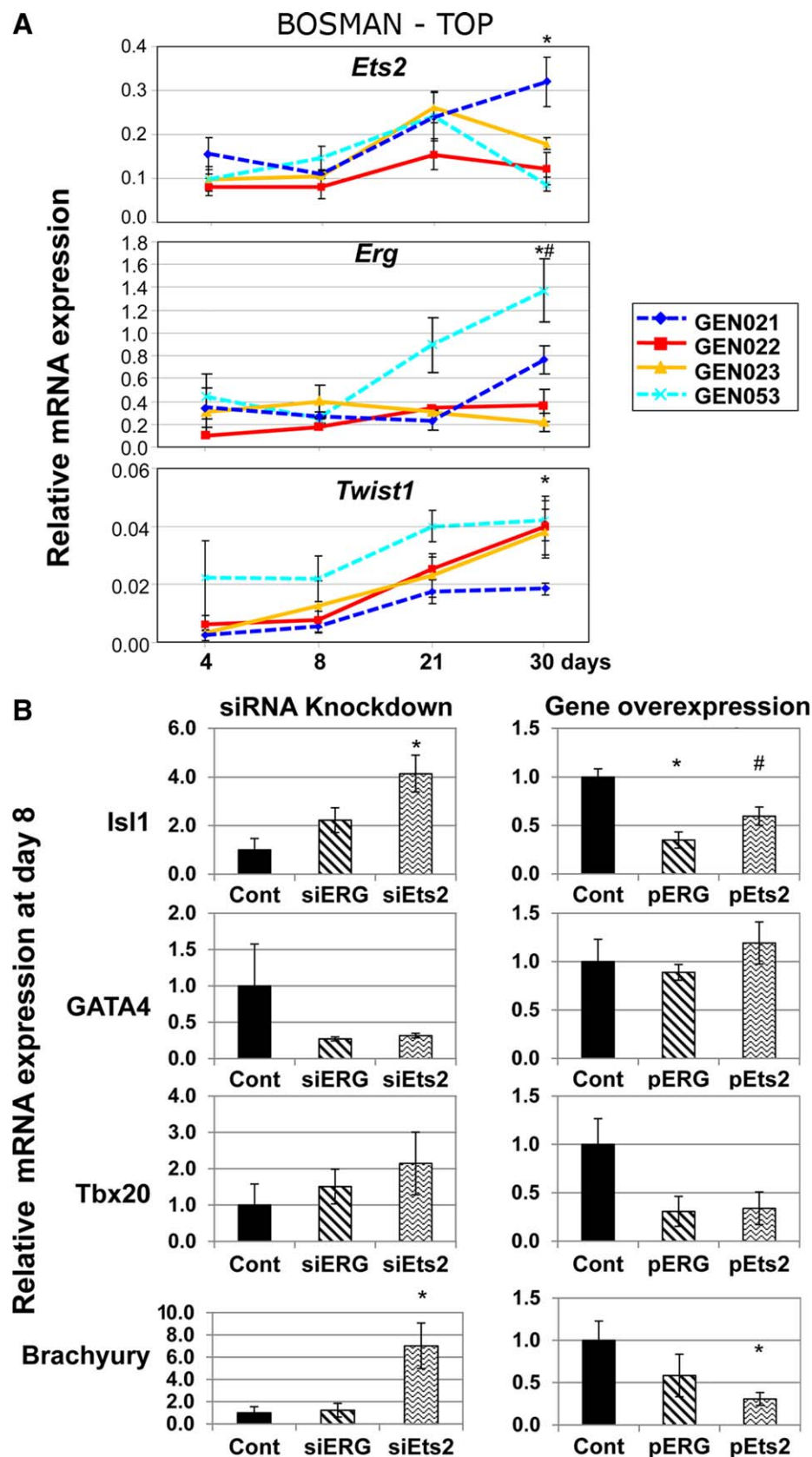
Figure 3. Expression of ETS2, ERG, TWIST1, and T-box transcription factors. **(A):** mRNA expression of ETS2, ERG, and TWIST1 ($n = 3–4$). **(B):** mRNA expression in differentiating human embryonic stem cell upon siRNA-mediated downregulation or plasmid-based overexpression of ETS2 or ERG ($n = 3–4$ independent experiments) *, $p < .05$; #, $p = .06$.
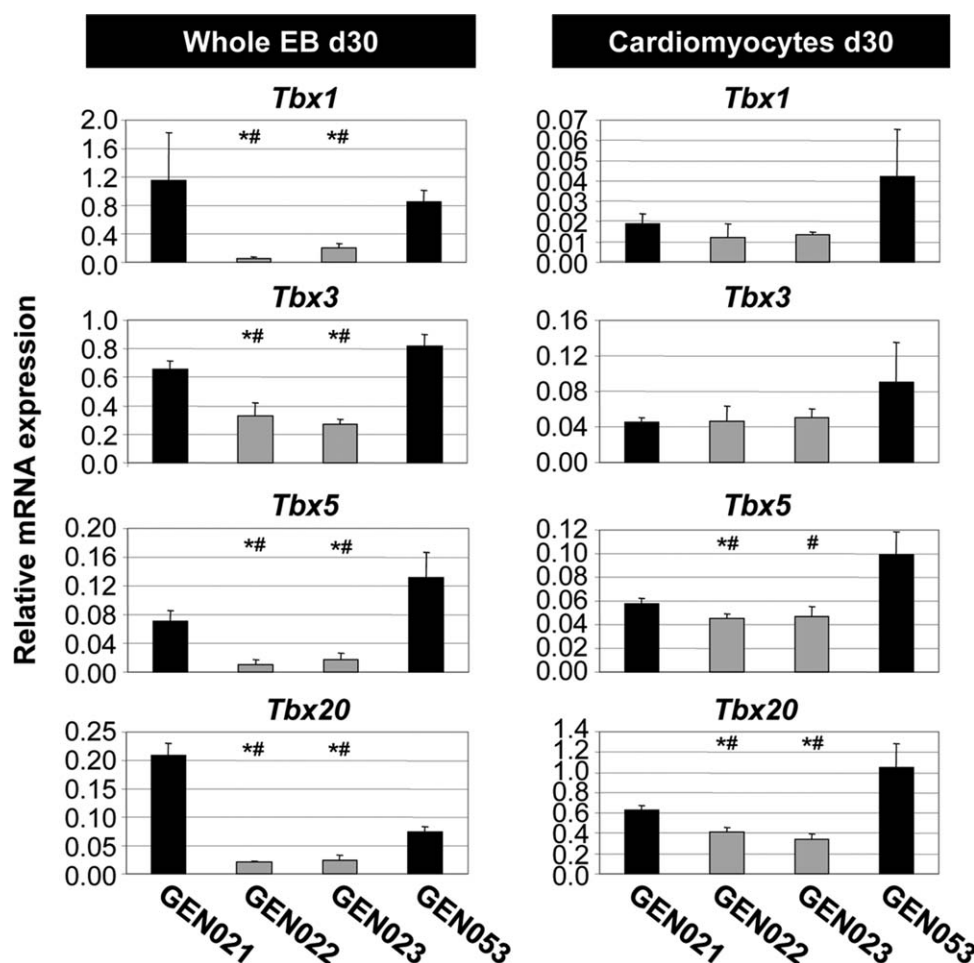
Figure 4. mRNA expression of T-box transcription factors at day 30 of differentiation in whole EBs (left) and in isolated cardiomyocytes (right) ($n = 3–4$). *, $p < .05$ (comparison to GEN021); #, $p < .05$ (comparison to GEN053). See also Supporting Information Figure S3. Abbreviation: EB, embryoid body.

Identification of CHD Candidate Genes on HSA21

In relation to candidate causative genes within the "CHD candidate region" present on HSA21 [31, 32], so far no specific gene(s) located on HSA21 have been directly associated with CHD in DS. Yet, from the recent literature, we identified both ETS2 and ERG as possible candidates underlying the cardiac phenotype in DS. ETS2 and ERG are both Ets-family transcription factors located in the CHD candidate region on HSA21 and have been either directly [33, 34], or indirectly [35, 36] associated with heart development. To determine whether ETS2 and ERG could be potential contributors in the cardiac phenotype observed in DS patients exhibiting CHD, we examined their expression levels during EB differentiation. Our results show a significant overexpression of ETS2 in GEN021 at d30 in comparison to both euploid controls (Fig. 3A), while ERG was significantly higher in both trisomic cells at d30 in comparison to euploid controls. This correlated with a reduced expression of TWIST1 (Fig. 3A) a transcription factor associated with cardiac cushion, valve development, and epithelial-mesenchymal transition (EMT). Indeed, TWIST1 has been shown to directly interact with members of the Ets family [37, 38], Ets factors being involved with EMT [39].

To examine the direct role of ETS2 and ERG in early mesodermal and cardiac differentiation, we performed in parallel a knockdown and overexpression study in differentiating EBs from GEN021 (siRNA knockdown) and GEN023 (expression vector overexpression). mRNA expression of ISL1, GATA4, TBX20, and BRACHYURY was examined by real-time PCR to determine if these two candidate genes play a role in the perturbations observed in the early differentiation patterns of T21-hESC. After validation of the knockdown/overexpression system (Supporting Information Fig. S3), we observed significant differences in the expression levels of ISL1 (Fig. 3B), both of which were correlative according to either overexpression or knockdown. Indeed, as expected, the ETS2/ERG knockdown in GEN021 led to increased ISL1 expression, while ETS2/ERG overexpression in GEN023 produced a corresponding significant decrease in ISL1 expression. The same response was observed with BRACHYURY, however only in the ETS2 treatment group (Fig. 3B). While GATA4 remained unchanged in any of the ETS2 and ERG overexpression treatment groups (Fig. 3B).

As T-box transcription factors have been shown to directly bind to both ETS2 and ERG, influencing their expression [40, 41], we next analyzed the expression of a selection of T-box transcription factors. Highly implicated in heart development and well associated with CHD, several T-box genes (TBX1,-3, −5, −20) were also found to be significantly overexpressed
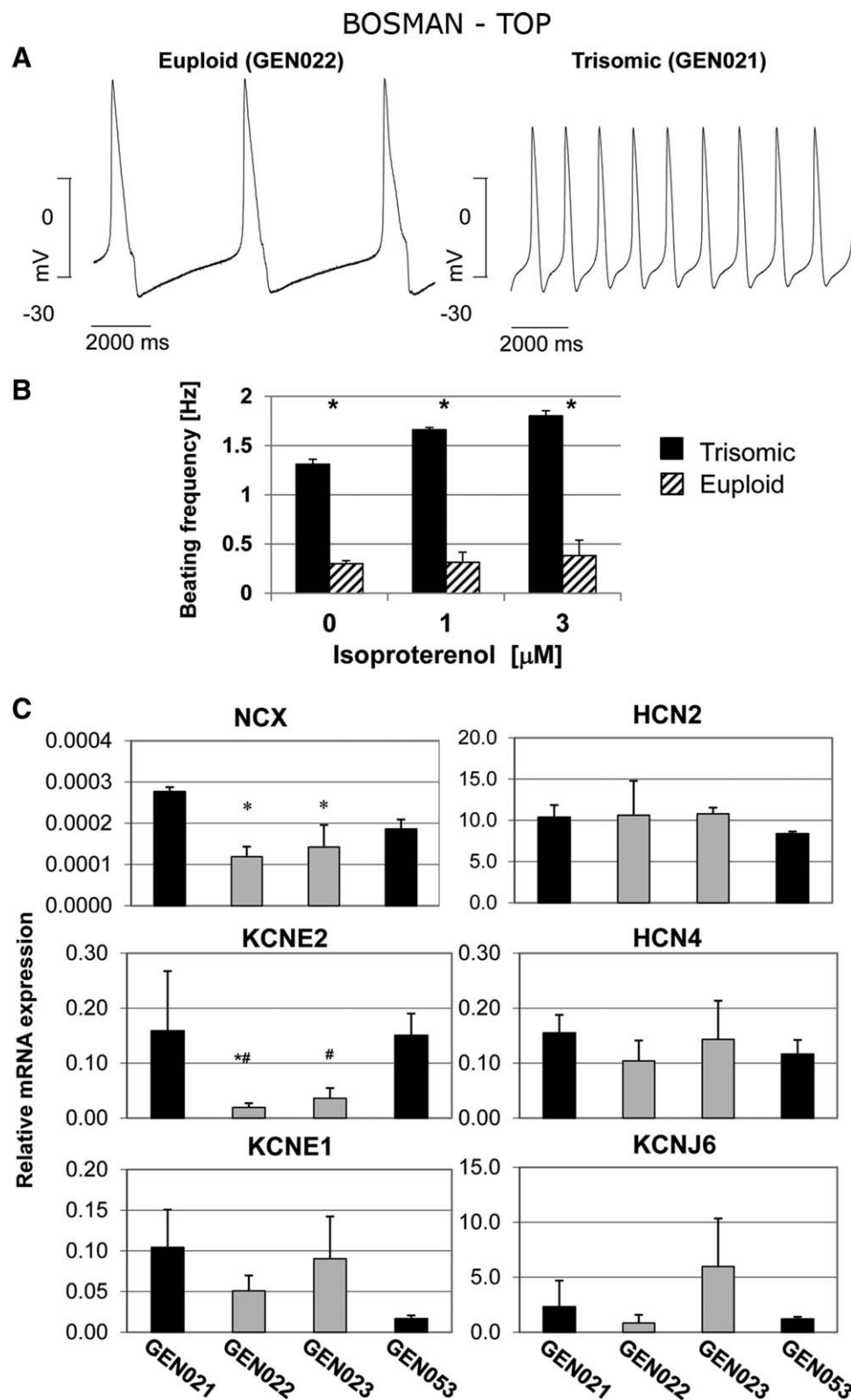
Figure 5. Analysis of electrophysiological differences in functional cardiomyocytes. **(A):** Multicellular recordings of action potentials (AP) in spontaneously beating clusters of cardiomyocytes at 160 ± 5 days of differentiation. Representative AP recordings in a 159-day old euploid and a 160-day old T21 beating cardiomyocyte cluster. **(B):** Dose-dependent increase of the beating frequency rate of T21 (GEN21) or euploid (GEN023) human embryonic stem cell-derived beating clusters from 40 to 80 days old in response to the βAR agonist isoproterenol (normalized data from $n = 8$–10 per condition; *, $p < .05$). **(C):** mRNA expression of the sodium calcium exchanger (NCX), as well as the channels KCNE2, KCNE1, HCN2, HCN4, and KCNJ6 in early embryonic body development ($n = 3$). Scheme: *, $p < .05$ (comparison to GEN021); #, $p < .05$ (comparison to GEN053).

Table 1. Analysis of the action potential parameters in euploid and T21 human embryonic stem cell-derived cardiomyocytes recorded at day 160 of culture

	Euploid (GEN022)	n	Trisomic (GEN021)	n	p
MDP (mV)	-35.6 ± 3.3	5	-33.5 ± 2.4	7	>0.05
APA (mV)	55.1 ± 6	5	47.2 ± 1.7	7	>0.05
APD30 (ms)	266.2 ± 26.4	5	164.4 ± 15.9	7	<0.001*
APD50 (ms)	315.8 ± 21.5	5	198 ± 14.6	7	<0.001*
APD70 (ms)	375.8 ± 23.8	5	228.4 ± 14.8	7	<0.001*
APD90 (ms)	504 ± 41.5	5	270.3 ± 17.5	7	<0.001*
$APD90_{cFram}$ (ms)	503.8 ± 41.5	5	270.3 ± 17.5	7	<0.001*
$APD90_{cFrid}$ (ms)	366.1 ± 24.5	5	288.9 ± 11.6	7	<0.05*
DDR (mV/ms)	0.0064 ± 0.0012	5	0.024 ± 0.0036	7	<0.001*
V_{max} (mV/ms)	2.28 ± 0.46	5	2.08 ± 0.26	7	>0.05
Freq (bpm)	23.6 ± 1.7	5	76.7 ± 6.6	7	<0.001*

Abbreviations: APA, AP amplitude; ADP30, 50, 70, and 90, AP duration needed to achieve 30%, 50%, 70%, and 90% of repolarization; $APD90_{cFram}$, corrected APD90 according to Framingham's formula; $APD90_{cFrid}$, corrected APD90 according to Fridericia's formula; bpm, beats per minute; DDR, diastolic depolarization rate; V_{max}, maximal upstroke velocity; Freq, frequency of spontaneous Aps; MDP, maximal diastolic potential.
*, $p < .05$

in T21 whole EB cultures at the d30 time point (Fig. 4, $n = 3$–4 independent experiments). However, in dissected beating cardiac clusters, only TBX5 (GEN053) and TBX20 (GEN021 and GEN053) were significantly overexpressed (Fig. 4; $n = 4$ independent experiments; *#, $p < .05$). We qualitatively confirmed TBX20 protein overexpression, specifically associated with

CHD [42], in GEN021 in comparison to GEN022 and GEN023 ($n = 2$ independent experiments, Supporting Information Fig. S4). Therefore, altogether, our results so far point to an overall perturbation in mesoderm and cardiac development, with identification of possible associated pathways involving ETS2, ERG, TWIST1, and T-box genes.
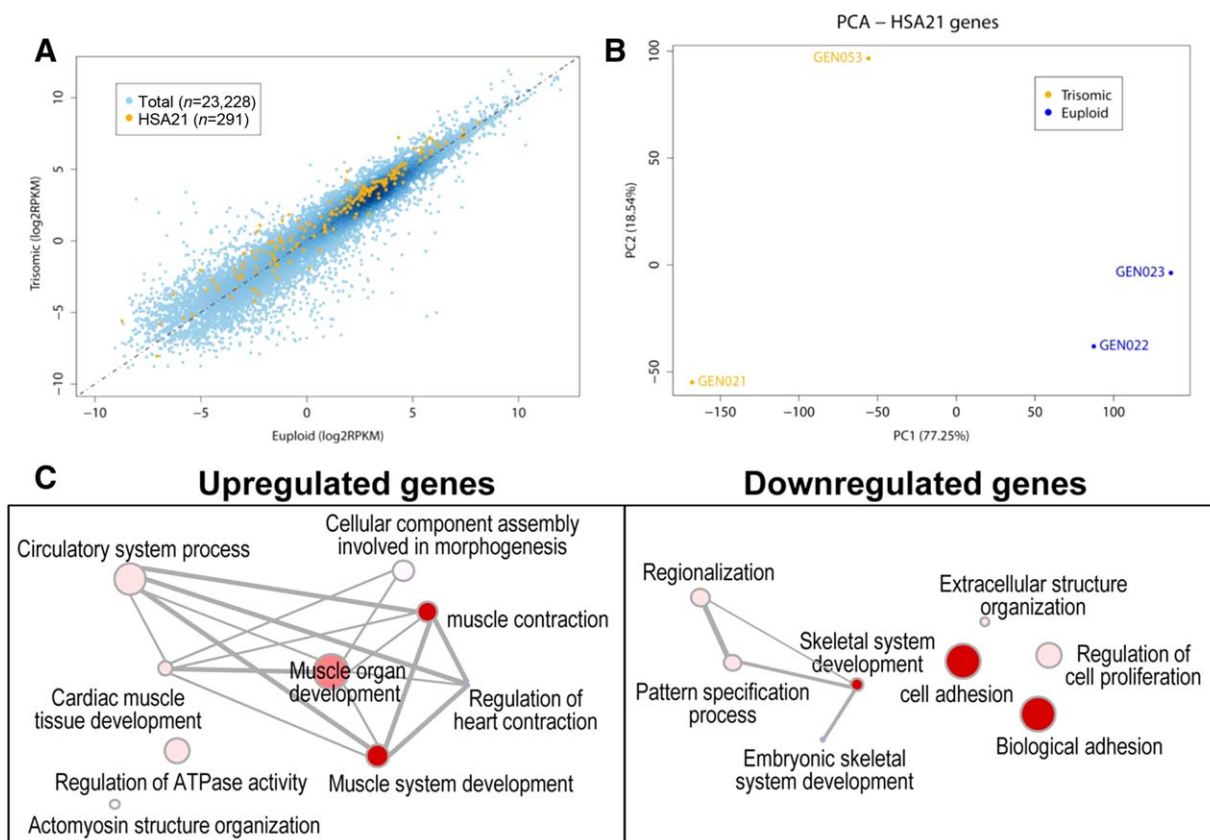

Figure 6. mRNA-Seq transcriptome analysis. **(A):** Comparison of the normalized gene expression levels between the euploid samples (GEN022 and GEN023, average log2 RPKM (reads per kilobase per million) value) and the trisomic samples (GEN021 and GEN053, average log2 RPKM value). Each blue dot represents one of the 23,228 expressed genes. The HSA21 genes are shown in orange. **(B):** PCA based on the RPKM values of HSA21 genes. The two first principal components (PC1 and PC2) are plotted. The contribution of each component is indicated in parenthesis. PC1 discriminates the euploid samples (in blue) from the trisomic samples (in orange). **(C):** REVIGO visualization of the biological processes significantly associated with the list of differentially expressed genes. The color and the size of each node represent the p value associated with the gene ontology (GO) term (dark red for small p values) and the frequency of the GO term in the human database, respectively. The degree of similarity between the terms is shown by the width of lines connecting the nodes. See also Supporting Information Figures S5, S6. Abrreviations: PCA, principal component analysis; PC, principal component.

Functional Differences Between Trisomic and Euploid Cardiomyocytes

To examine the functional characteristics of hESC-derived cardiomyocytes, we performed multicellular recordings of action potentials (AP) in spontaneously beating clusters of sibling cardiomyocytes. AP profiles detected from T21 and euploid cardiomyocytes up to 160 ± 5 days of differentiation differed substantially, as evident from representative recordings shown in Fig. 5A. In particular, frequency of spontaneous beating was significantly higher in T21 cardiomyocytes (Table 1), together with a significantly faster diastolic depolarization rate in T21 compared to euploid cardiomyocytes. Additionally, AP profiles revealed a substantially shorter duration of repolarization in T21, as shown by measurements of time needed to achieve 30%, 50%, 70%, and 90% of repolarization. The difference in AP duration in euploid and trisomic cardiomyocytes was maintained after correction for beating rate. Other AP parameters, namely maximal diastolic potential, AP amplitude, and maximal upstroke velocity were not different in T21 and euploid cardiomyocytes. Overall, the above functional data show a global perturbation of electrophysiological properties in T21 cardiomyocytes, pointing the attention to two different parameters of AP, namely duration and spontaneous frequency. In addition, using multielectrode arrays, we also confirmed a higher AP frequency in trisomic beating clusters upon submaximal beta-adrenergic stimulation by isoproterenol, compared to euploid clusters (Fig. 5B).

Candidate genes which may underlie the observed electrophysiological differences were examined for their expression profiles at d30 by qPCR. These include ion channel genes located on HSA21 (KCNE1, KCNE2, KCNJ6), HCN channels (HCN2, HCN4), and the sodium-calcium exchanger (NCX). Significant differences in expression levels were observed in both NCX and KCNE2 between GEN021 and its sibling controls (Fig. 5C).

Whole Transcriptome Analysis of Day 60 Cardiomyocytes Derived from hESC Using mRNA-Sequencing

To further examine specific differences in cardiomyocytes generated from both T21 and euploid hESC, we performed next generation sequencing on isolated beating cardiomyocytes (CM) at day 60 of differentiation. We first assessed the expression level of each gene by calculating the exon coverage of the longest transcript and by normalizing the number of reads to RPKM. In total, 23,228 genes were expressed, including 291 genes on HSA21. As expected, most of the HSA21 genes were overexpressed in the trisomic samples compared to the normal samples (Fig. 6A; Supporting Information Fig. S5). Clustering analysis based on HSA21 gene expression showed a clear separation of the two groups (Supporting Information Fig. S5). In the PCA, the first principal component (PC1) clearly discriminates the euploid from the trisomic group and explains most of the variance between the samples (77.25%, Fig. 6B). We next assessed the differential expression between the euploid and the trisomic samples using the edgeR and DESeq programs [27]. In total, 501 genes were predicted as differentially expressed by both packages (FDR <1% in edgeR and DESeq). Among them, 280 genes were found upregulated in the trisomic group and 221 genes downregulated (Supporting Information Table 2).

To check if specific biological processes were overrepresented in the 501 differentially expressed genes, we performed a functional annotation analysis using DAVID. Interestingly, the 221 genes downregulated in the trisomic samples were mainly associated with developmental terms and cellular adhesion processes (Fig. 6C; Supporting Information Fig. S6). The analysis of the 280 upregulated genes however, revealed biological terms almost exclusively related to muscle and heart contraction or development processes (Fig. 6C). Importantly, this list was also enriched for genes involved in five signaling pathways, all related to the heart function: dilated cardiomyopathy (19 genes, $p = 5.15E\text{-}13$), hypertrophic cardiomyopathy (16 genes, $p = 5.67E\text{-}10$), cardiac muscle contraction (12 genes, $p = 5.07E\text{-}06$), calcium signaling pathway (16 genes, $p = 1.79E\text{-}05$), and arrhythmogenic right ventricular cardiomyopathy (10 genes, $p = 3.86E\text{-}04$). Interestingly, among the 33 upregulated genes involved in these pathways, 3 genes were common to all of them: CACNA1D, RYR2, and SLC8A1, that encode for the L-type, voltage-dependent calcium channel, alpha 1D subunit, the ryanodine receptor 2 (cardiac), and the sodium/calcium exchanger, respectively. Notably, these genes are all associated with calcium signaling and excitation-contraction coupling in cardiomyocytes (Supporting Information Fig. S6).

DISCUSSION

In this study, using a sibling hESC model for recapitulating early cardiogenesis in DS, we have uncovered several genes involved in early mesodermal and SHF development which are differentially expressed in T21-hESC in comparison to euploid hESC. Of note, we identified two genes, ETS2 and ERG, located on HSA21 and shown to be associated to EMT and cardiac cushion development, whose overexpression may contribute to the CHD observed in DS. Finally, in T21 cardiomyocytes we identified significant functional differences and a cardiomyocyte-specific disease-type phenotype.

Using sibling hESC lines allows the assignation of very small differences in differentiation and development to the disease itself, as opposed to differences in genetic/epigenetic background or in derivation/culturing conditions. The latter are otherwise emphasized when comparing genetically unrelated pluripotent stem cell lines with varying intrinsic differentiation capacities, genomic stability, and epigenetic patterning [30]. Indeed, our disease model of DS has allowed the identification of expression differences only in the sibling T21-hESC (e.g., BRACHYURY), while for some other genes, both T21-hESC were concurrently significantly higher or lower than the euploid controls (e.g., GATA4 and ISL1, respectively). We therefore suggest that small but biologically significant gene expression differences may only be uncovered in genetically related pluripotent lines, in particular for complex genetic diseases such as trisomies. Significant expression differences between unrelated T21-hESC would require a larger number of lines to definitively observe the effect of genes more greatly affected by aneuploidy.

CHD are known to be associated with altered expression or mutations in several genes, including: NKX2–5 [43], GATA4 [44], ISL1 [45], NOTCH1 [46], as well as with several T-box genes, including: TBX1 [47], TBX5 [48], and TBX20 [42, 49]. Here we have identified several important transcription factors differentially expressed at specific time points in the

©AlphaMed Press 2015

trisomic cells, in comparison to their euploid counterparts. Genes involved in early cardiac development such as NKX2–5, MESP1, GATA4, β-catenin, NOTCH1, WNT11, and ISL1 have shown multiple differences in their mRNA expression levels, with ISL1 and GATA4 showing the most clear differential expression, also observed at the protein level by FACS analysis. In particular, genes associated with the development of early mesoderm and the SHF were mainly under-expressed at early time points of differentiation.

We have shown that two important early mesodermal/cardiac progenitor genes—BRACHYURY (required for the formation of the primitive streak) and MESP1 (one of the earliest markers of the heart, exclusively expressed in all cardiovascular progenitors [50])—are less expressed at d8 in trisomic cells, a point in development which would have major implications for mesodermal lineage development. Additionally, we have shown that WNT11 and WNT3A were also less expressed in T21 cells. Wnt signaling plays an important role in cardiogenesis via canonical Wnt/β-catenin pathway and noncanonical Wnt/Ca^{2+} and JNK pathways [51]. Specifically, the noncanonical WNT11, a marker of the outflow tract (OFT) and the only Wnt whose expression overlaps with the pre-cardiac mesoderm [52], was decreased, likely due to a reduction in ISL1 and/or in ISL1-expressing cells.

ISL1$^+$ progenitors give rise to the SHF, which includes the OFT as well as a majority of cells in both the right ventricle and the atria, and some cells within the left ventricle [53]. Inactivation, or underexpression, of ISL1 is thus expected to affect OFT and right ventricle formation, resulting in perturbed heart development. Of particular note, Wnt signaling pathway is known to influence the development of SHF with knockout studies showing hypoplasia of SHF structures, including the interventricular septae. Moreover, abnormal heart formation has been observed when the close relationship between β-catenin and ISL1 expressions are affected [54–57], as what was observed in our differentiation experiments.

Interestingly, we have identified expression changes in ETS2 and ERG, members of the Ets family of transcription factors, both located on human HSA21, specifically in the candidate DS region for CHD [58]. By reducing their mRNA levels in early differentiating trisomic cells or increasing them in euploid cells we could re-establish, or respectively enhance, the levels of the early mesoderm marker BRACHYURY and of downstream effectors such as ISL1 and GATA4. In chick embryos, it was observed that high levels of ETS2 mRNA are expressed in the atrioventricular canal (AVC) and OFT regions [59]—the regions which undergo the EMT [60]. It is hypothesized that during this process, or in the perturbation of EMT, septal and valvular defects arise, thus making disruptions in this process a possible candidate pathway for CHD in DS. As is the case particularly for WNT11 [41], many cardiac genes contain Ets binding sites in their promoters including cardiac α-MyHC, β-MyHC, MLC-2, cardiac troponin T, cardiac troponins C and I, ANF, α-cardiac actin [61], and also basic helix-loop-helix transcription factor TWIST1 [37, 38]. In the heart, TWIST1 is expressed in the cardiac cushions [62] and has been associated with migration, differentiation, and proliferation of mesenchymal populations, including metastatic dissemination of cancer cells through its EMT induction properties. Of note, TWIST1 has been shown to coimmunoprecipitate with ETS2 [63] and to coexpress with a number of T-box genes in other mesenchymal

derived tissues, such as the developing limbs [64]. Whether TWIST1/T-box interactions act in a common developmental pathway remains to be established.

We propose that due to the overexpression of ETS2 and ERG in early heart development as a result of the extra chromosome in DS, septal formation is disturbed. This may occur as a consequence of the overexpression of ETS and ERG directly, or indirectly, by the overexpression of TBX20, or other T-box genes. Indeed, our observation of increased expression of many T-box genes (TBX1, -3, -5, and -20), suggests an overall disturbance in normal cardiogenesis, possibly altogether leading to a phenotype of CHD. This is in line with the reported effects of TBX differential expression in cardiac malformations [47, 48]. For instance, overexpression of TBX5 leads to a loss of ventricular septum and atrioventricular cushions (AC) cushions in mice [65]. Similarly, differential expression of TBX20 has been shown to be involved in CHD such as atrioventricular septal defects, ventricular septal defects, and tetralogy of fallot [42, 66, 67].

Finally, our mRNA-seq analysis reveals an extensive dysregulation of different genes related to muscle and heart contraction, which hold potential consequences at a functional level. Indeed, our electrophysiological measurements show a well-defined modification of the functional phenotype in differentiated cardiomyocytes. Specifically, in euploid cardiomyocytes, AP frequency and morphology are similar to those previously described in mature hESC cardiomyocytes maintained in long-term culture [22, 29], suggesting the attainment of a similar maturation grade. Conversely, in T21-cardiomyocytes, both parameters recall those observed in immature cardiomyocytes, suggesting the presence of abnormalities in their functional maturation. This process is closely mediated by diverse ion channels and regulatory proteins that control and shape distinct phases of AP [68, 69]. In particular, the elevated beating frequency and the fast diastolic depolarization rate in T21-cardiomyocytes are suggestive of elevated functional expression of ion currents, namely; I_f—or HCN-mediated, sodium-calcium exchanger and L-type calcium currents that we previously reported to positively control these parameters in hESC-derived cardiomyocytes [29, 69]. This observation is in line with our gene expression analysis showing a robust overexpression of CACNA1D and SLC8A1, encoding for the L-type, voltage-dependent calcium channel, alpha 1D subunit, and the sodium/calcium exchanger, respectively, in T21 compared to euploid cardiomyocytes. Additionally, the overexpression of RYR2 receptor in T21-cardiomyocytes may potentially further sustain the elevated beating frequency detected in these cells, in agreement with data showing a key role of ryanodine receptors in driving pacemaker function of spontaneous beating cells [70]. Of note, the differences in AP frequency detected in our model are in line with the higher heart rate values documented in trisomic embryos [71, 72]. Taken together, these results contribute to the concept of a global derangement of electrophysiological maturation attained by T21-cardiomyocytes. Whether this observation encompasses other functional properties of T21-cardiomyocytes, namely contraction-relaxation as suggested by gene expression data, is an interesting perspective of future investigations. It is also interesting to speculate that the cause of the high number of spontaneous miscarriages in trisomy 21 fetuses ($\sim$75% [73]) may be the consequence of abnormalities in cardiomyocyte function, thus preventing their survival to term. Further analysis is warranted in order to determine if this may truly be the case.

Conclusion

Here we show that hESC carrying trisomy 21 exhibit both developmental and functional differences upon differentiation to cardiomyocytes. Furthermore, studying complex diseases such as Down syndrome using sibling hESC lines allows a more sensitive approach to uncovering underlying perturbations in early development.

The Victor Chang Cardiac Research Institute does not engage in, nor does it condone, the destruction of human embryos for research.

Author Contributions

A.B.: conception and design, collection and/or assembly of data, data analysis and interpretation, and manuscript writing; A.L.: data analysis and interpretation and manuscript writing; L.S.: collection and/or assembly of data and manuscript writing; M.D.L., F.R., F.S., M.G., and V.T.: collection and/or assembly of data; R.K., M.Z.: data analysis and interpretation; B.D.: provision of study material or patients; O.H.: financial support and final approval of manuscript; S.A.: conception and design, financial support, and final approval of manuscript; M.J.: conception and design, data analysis and interpretation, financial support, and manuscript writing.

Disclosure of Potential Conflicts of Interest

The authors indicate no potential conflicts of interest.

References

1 Letourneau A, Antonarakis SE. Genomic determinants in the phenotypic variability of Down syndrome. Progr Brain Res 2012;197:15–28.

2 Reeves RH, Baxter LL, Richtsmeier JT. Too much of a good thing: Mechanisms of gene action in Down syndrome. Trends Genet 2001;17:83–88.

3 Patterson D, Costa AC. Down syndrome and genetics—A case of linked histories. Nat Rev Genet 2005;6:137–147.

4 Antonarakis SE, Lyle R, Dermitzakis ET, et al. Chromosome 21 and down syndrome: From genomics to pathophysiology. Nat Rev Genet 2004;5:725–738.

5 Sailani MR, Makrythanasis P, Valsesia A et al. The complex SNP and CNV genetic architecture of the increased risk of congenital heart defects in Down syndrome. Genome Res 2013;23:1410–1421.

6 Williams AD, Mjaatvedt CH, Moore CS. Characterization of the cardiac phenotype in neonatal Ts65Dn mice. Dev Dyn 2008;237:426–435.

7 Sommer CA, Henrique-Silva F. Trisomy 21 and Down syndrome: A short review. Braz J Biol 2008;68:447–452.

8 Kuhn DE, Nuovo GJ, Martin MM et al. Human chromosome 21-derived miRNAs are overexpressed in down syndrome brains and hearts. Biochem Biophys Res Commun 2008;370:473–477.

9 Li CM, Guo M, Salas M et al. Cell type-specific over-expression of chromosome 21 genes in fibroblasts and fetal hearts with trisomy 21. BMC Med Genet 2006;7:24.

10 Prandini P, Deutsch S, Lyle R et al. Natural gene-expression variation in Down syndrome modulates the outcome of gene-dosage imbalance. Am J Hum Genet 2007;81:252–263.

11 Wang Y, Mulligan C, Denyer G et al. Quantitative proteomic characterisation of a mouse embryonic stem cell model of Down syndrome. Mol Cell Proteomics 2008;8:585–595.

12 Lu HE, Yang YC, Chen SM et al. Modeling neurogenesis impairment in down syndrome with induced pluripotent stem cells from Trisomy 21 amniotic fluid cells. Exp Cell Res 2013;319:498–505.

13 Biancotti JC, Narwani K, Buehler N et al. Human embryonic stem cells as models for aneuploid chromosomal syndromes. Stem Cells 2010;28:1530–1540.

14 Briggs JA, Sun J, Shepherd J et al. Integration-free induced pluripotent stem cells model genetic and neural developmental features of Down Syndrome etiology. Stem Cells 2013;31:467–478.

15 Chou ST, Byrska-Bishop M, Tober JM et al. Trisomy 21-associated defects in human primitive hematopoiesis revealed through induced pluripotent stem cells. Proc Natl Acad Sci USA 2012;109:17573–17578.

16 Li LB, Chang KH, Wang PR et al. Trisomy correction in down syndrome induced pluripotent stem cells. Cell Stem Cell 2012;11:615–619.

17 Letourneau A, Santoni FA, Bonilla X et al. Domains of genome-wide gene expression dysregulation in Down's syndrome. Nature 2014;508:345–350.

18 Osafune K, Caron L, Borowiak M et al. Marked differences in differentiation propensity among human embryonic stem cell lines. Nat Biotechnol 2008;26:313–315.

19 Jauniaux E, Gavrill P, Khun P et al. Fetal heart rate and umbilico-placental Doppler flow velocity waveforms in early pregnancies with a chromosomal abnormality and/or an increased nuchal translucency thickness. Hum Reprod 1996;11:435–439.

20 Henman M, Catt JW, Wood T et al. Elective transfer of single fresh blastocysts and later transfer of cryostored blastocysts reduces the twin pregnancy rate and can improve the in vitro fertilization live birth rate in younger women. Fertil Steril 2005;84:1620–1627.

21 Bradley CK, Chami O, Peura TT et al. Derivation of three new human embryonic stem cell lines. In Vitro Cell Dev Biol Anim 2010;46:294–299.

22 Bettiol E, Sartiani L, Chicha L et al. Fetal bovine serum enables cardiac differentiation of human embryonic stem cells. Differentiation 2007;75:669–681.

23 Feki A, Bosman A, Dubuisson JB et al. Derivation of the first Swiss human embryonic stem cell line from a single blastomere of an arrested four-cell stage embryo. Swiss Med Wkly 2008;138:540–550.

24 Sandoval J, Heyn HA, Moran S et al. Validation of a DNA methylation microarray for 450,000 CpG sites in the human genome. Epigenetics 2011;6.

25 Li H, Durbin R. Fast and accurate short read alignment with Burrows-Wheeler transform. Bioinformatics 2009;25:1754–1760.

26 Robinson MD, McCarthy DJ, Smyth GK. EdgeR: A Bioconductor package for differential expression analysis of digital gene expression data. Bioinformatics 2010;26:139–140.

27 Anders S, Huber W. Differential expression analysis for sequence count data. Genome Biol 2010;11:R106.

28 Huang da W, Sherman BT, Lempicki RA. Bioinformatics enrichment tools: Paths toward the comprehensive functional analysis of large gene lists. Nucleic Acids Res 2009;37:1–13.

29 Sartiani L, Bettiol E, Stillitano F et al. Developmental changes in cardiomyocytes differentiated from human embryonic stem cells: A molecular and electrophysiological approach. Stem Cells 2007;25:1136–1144.

30 Bock C, Kiskinis E, Verstappen G et al. Reference maps of Human ES and iPS cell variation enable high-throughput characterization of pluripotent cell lines. Cell 2010;144:439–452.

31 Korbel JO, Tirosh-Wagner T, Urban AE et al. The genetic architecture of Down syndrome phenotypes revealed by high-resolution analysis of human segmental trisomies. Proc Natl Acad Sci USA 2009;106:12031–12036.

32 Lyle R, Bena F, Gagos S et al. Genotype-phenotype correlations in Down syndrome identified by array CGH in 30 cases of partial trisomy and partial monosomy chromosome 21. Eur J Hum Genet 2009;17:454–466.

33 Vijayaraj P, Le Bras A, Mitchell N et al. Erg is a crucial regulator of endocardial-mesenchymal transformation during cardiac valve morphogenesis. Development 2012;139:3973–3985.

34 Schachterle W, Rojas A, Xu SM et al. ETS-dependent regulation of a distal Gata4 cardiac enhancer. Dev Biol 2012;361:439–449.

35 Polydorou C, Georgiades P. Ets2-dependent trophoblast signalling is required for gastrulation progression after primitive streak initiation. Nat Commun 2013;4:1658.

36 Islas JF, Liu Y, Weng KC et al. Transcription factors ETS2 and MESP1 transdifferentiate human dermal fibroblasts into cardiac progenitors. Proc Natl Acad Sci USA 2012;109:13016–13021.

37 Kathuria H, Wong K-k, Carretero J et al. ETS-1 regulates Twist-1 expression in non-small cell lung cancer (NSCLC) progression and metastasis. Am J Respir Crit Care Med 2011;183:A4049.

38 Wong KK, Carretero J, Ramirez MI et al. Increased Ets-1 positively correlates with Twist1 expression in mouse non-small cell lung cancer (NSCLC) progression and metastases. Am J Respir Crit Care Med 2010;181:A2054.

39 Hsu T, Trojanowska M, Watson DK. Ets proteins in biological control and cancer. J Cell Biochem 2004;91:896–903.

40 Ma L, Li J, Liu Y et al. Novel and functional variants within the TBX18 gene promoter in ventricular septal defects. Mol Cell Biochem 2013;382:121–126.

41 Mochmann LH, Bock J, Ortiz-Tanchez J et al. Genome-wide screen reveals WNT11, a non-canonical WNT gene, as a direct target of ETS transcription factor ERG. Oncogene 2011;30:2044–2056.

42 Kirk EP, Sunde M, Costa MW et al. Mutations in cardiac T-box factor gene TBX20 are associated with diverse cardiac pathologies, including defects of septation and valvulogenesis and cardiomyopathy. Am J Hum Genet 2007;81:280–291.

43 Schott JJ, Benson DW, Basson CT et al. Congenital heart disease caused by mutations in the transcription factor NKX2–5. Science 1998;281:108–111.

44 Garg V, Kathiriya IS, Barnes R et al. GATA4 mutations cause human congenital heart defects and reveal an interaction with TBX5. Nature 2003;424:443–447.

45 Stevens KN, Hakonarson H, Kim CE et al. Common variation in ISL1 confers genetic susceptibility for human congenital heart disease. PLoS One 2010;5:e10855.

46 Nemir M, Pedrazzini T. Functional role of Notch signaling in the developing and postnatal heart. J Mol Cell Cardiol 2008;45:495–504.

47 Liao J, Aggarwal VS, Nowotschin S et al. Identification of downstream genetic pathways of Tbx1 in the second heart field. Dev Biol 2008;316:524–537.

48 Basson CT, Huang T, Lin RC et al. Different TBX5 interactions in heart and limb defined by Holt-Oram syndrome mutations. Proc Natl Acad Sci USA 1999;96:2919–2924.

49 Cai CL, Zhou W, Yang L et al. T-box genes coordinate regional rates of proliferation and regional specification during cardiogenesis. Development 2005;132:2475–2487.

50 Saga Y, Kitajima S, Miyagawa-Tomita S. Mesp1 expression is the earliest sign of cardiovascular development. Trends Cardiovasc Med 2000;10:345–352.

51 Terami H, Hidaka K, Katsumata T et al. Wnt11 facilitates embryonic stem cell differentiation to Nkx2.5-positive cardiomyocytes. Biochem Biophys Res Commun 2004;325:968–975.

52 Eisenberg CA, Eisenberg LM. WNT11 promotes cardiac tissue formation of early mesoderm. Dev Dyn 1999;216:45–58.

53 Cai CL, Liang X, Shi Y et al. Isl1 identifies a cardiac progenitor population that proliferates prior to differentiation and contributes a majority of cells to the heart. Dev Cell 2003;5:877–889.

54 Cohen ED, Wang Z, Lepore JJ et al. Wnt/beta-catenin signaling promotes expansion of Isl-1-positive cardiac progenitor cells through regulation of FGF signaling. J Clin Invest 2007;117:1794–1804.

55 Kwon C, Qian L, Cheng P et al. A regulatory pathway involving Notch1/beta-catenin/Isl1 determines cardiac progenitor cell fate. Nat Cell Biol 2009;11:951–957.

56 Lin L, Cui L, Zhou W et al. Beta-catenin directly regulates Islet1 expression in cardiovascular progenitors and is required for multiple aspects of cardiogenesis. Proc Natl Acad Sci USA 2007;104:9313–9318.

57 Qyang Y, Martin-Puig S, Chiravuri M et al. The renewal and differentiation of Isl1+ cardiovascular progenitors are controlled by a Wnt/beta-catenin pathway. Cell Stem Cell 2007;1:165–179.

58 Barlow GM, Chen XN, Shi ZY et al. Down syndrome congenital heart disease: A narrowed region and a candidate gene. Genet Med 2001;3:91–101.

59 Majka SM, McGuire PG. Regulation of urokinase expression in the developing avian heart: A role for the Ets-2 transcription factor. Mech Dev 1997;68:127–137.

60 Person AD, Klewer SE, Runyan RB. Cell biology of cardiac cushion development. Int Rev Cytol 2005;243:287–335.

61 Gupta M, Zak R, Libermann TA et al. Tissue-restricted expression of the cardiac alpha-myosin heavy chain gene is controlled by a downstream repressor element containing a palindrome of two ets-binding sites. Mol Cell Biol 1998;18:7243–7258.

62 Shelton EL, Yutzey KE. Twist1 function in endocardial cushion cell proliferation, migration, and differentiation during heart valve development. Dev Biol 2008;317:282–295.

63 Ansieau S, Bastid J, Doreau A et al. Induction of EMT by twist proteins as a collateral effect of tumor-promoting inactivation of premature senescence. Cancer Cell 2008;14:79–89.

64 O'Rourke MP, Soo K, Behringer RR et al. Twist plays an essential role in FGF and SHH signal transduction during mouse limb development. Dev Biol 2002;248:143–156.

65 Greulich F, Rudat C, Kispert A. Mechanisms of T-box gene function in the developing heart. Cardiovasc Res 2011;91:212–222.

66 Hammer S, Toenjes M, Lange M et al. Characterization of TBX20 in human hearts and its regulation by TFAP2. J Cell Biochem 2008;104:1022–1033.

67 Takeuchi JK, Mileikovskaia M, Koshiba-Takeuchi K et al. Tbx20 dose-dependently regulates transcription factor networks required for mouse heart and motoneuron development. Development 2005;132:2463–2474.

68 Bosman A, Sartiani L, Spinelli V et al. Molecular and functional evidence of HCN4 and caveolin-3 interaction during cardiomyocyte differentiation from human embryonic stem cells. Stem Cells Dev 2013;22:1717–1727.

69 Paci M, Sartiani L, Del Lungo M et al. Mathematical modelling of the action potential of human embryonic stem cell derived cardiomyocytes. Biomed Eng Online 2012;11:61.

70 Vinogradova TM, Maltsev VA, Bogdanov KY et al. Rhythmic Ca2+ oscillations drive sinoatrial nodal cell pacemaker function to make the heart tick. Ann N Y Acad Sci 2005;1047:138–156.

71 Hyett JA, Noble PL, Snijders RJ et al. Fetal heart rate in trisomy 21 and other chromosomal abnormalities at 10–14 weeks of gestation. Ultrasound Obstet Gynecol 1996;7:239–244.

72 Liao AW, Snijders R, Geerts L et al. Fetal heart rate in chromosomally abnormal fetuses. Ultrasound Obstet Gynecol 2000;16:610–613.

73 Spencer K. What is the true fetal loss rate in pregnancies affected by trisomy 21 and how does this influence whether first trimester detection rates are superior to those in the second trimester? Prenatal Diagnosis 2001;21:788–789.

See www.StemCells.com for supporting information available online.